Analytica Chimica Acta 847 (2014) 37–43

Contents lists available at ScienceDirect

Analytica Chimica Acta

journal homepage: www.elsevier.com/locate/aca

Multiplexed electrochemical immunoassay using streptavidin/nanogold/carbon nanohorn as a signal tag to induce silver deposition

Changrong Zhao [a,b,1], Jie Wu [a,1], Huangxian Ju [a,*], Feng Yan [c,*]

[a] State Key Laboratory of Analytical Chemistry for Life Science, Department of Chemistry, Nanjing University, Nanjing 210093, PR China
[b] School of Environmental Science and Public Health, Wenzhou Medical College, Wenzhou 325035, PR China
[c] Jiangsu Institute of Cancer Prevention and Cure, Nanjing 210009, PR China

HIGHLIGHTS

- Streptavidin functionalized nanogold/carbon nanohorn as a new common tracing tag is synthesized.
- This tag can recognize the biotinylated signal antibodies to perform multiplexed immunoassay.
- Coupling with the nanomaterial-promoted silver enhancement amplifies the signal and greatly improves the sensitivity of immunoassay.
- This method is simple and low-cost, and exhibits wide concentration range and acceptable, reproducibility, stability and accuracy.

GRAPHICAL ABSTRACT

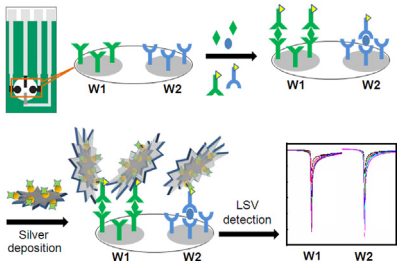

ARTICLE INFO

Article history:
Received 9 July 2013
Received in revised form 21 July 2014
Accepted 22 July 2014
Available online 24 July 2014

Keywords:
Electrochemical sensor
Immunosensor
Multiplexed immunoassay
Signal amplification
Silver enhancement
Carbon nanohorn

ABSTRACT

An ultrasensitive multiplexed immunoassay method was developed by using streptavidin/nanogold/carbon nanohorn (SA/Au/CNH) as a novel signal tag to induce silver enhancement for signal amplification. The Au/CNH was prepared by in situ growth of nanogold on carboxylated CNH and functionalized with streptavidin. The SA/Au/CNH showed well dispersibility in physiological buffer and could sever as a common tracing tag to recognize biotinylated signal antibody. The immunosensor array was prepared on disposable screen-printed electrodes. Through sandwich-type immunoreaction and biotin-streptavidin affinity reaction, the SA/Au/CNH tag was captured on the immunoconjugates to induce silver deposition and amplify the electrochemical stripping signals. Using α-fetoprotein and carcinoembryonic antigen as model analytes, the proposed method showed wide linear ranges with the detection limits down to 0.024 pg mL^{-1} and 0.032 pg mL^{-1}, respectively, and eliminated completely signal cross-talk between adjacent immunosensors. It provided a convenient, high-efficient and ultrasensitive electrochemical detection route for biological analytes, showing great potential in clinical application.

1. Introduction

Due to the significant positive correlation between the levels of tumor biomarkers in serum/tissue and the stages of tumors, accurate and sensitive multiplexed detection of biomarkers plays

* Corresponding authors. Tel.: +86 25 83593593.
E-mail addresses: hxju@nju.edu.cn (H. Ju), yanfeng2007@sohu.com (F. Yan).
[1] These authors contributed equally to this work.

http://dx.doi.org/10.1016/j.aca.2014.07.035
0003-2670/

an essential role in reliable screen and diagnosis of cancer in the early stage [1,2]. Various immunosensor arrays combining with electrochemical [3–6] and optical [7–10] readout have been designed for simultaneous detection of multiplex analytes. Owing to the unique advantages of easy preparation, low cost, high sensitivity and good portability [11–13], electrochemical sensor array, especially those fabricated on the disposable screen-printed electrode strips, have gained considerable attention for their potential application in point-of-care treatment [5].

Commonly, electrochemical immunoassay uses an enzyme labeled signal antibody coupling with an enzymatic reaction to trace the immunosensing events [3–5]. With the development of nanoscience and nanotechnology, various nanomaterial-based tracing tags have been designed to amplify the electrochemical signal and develop ultrasensitive immunoassay methods [14]. The most popular strategy is performed by conjugating large amounts of signal molecules such as enzymes [15,16], electroactive molecules [17] and metallic nanoparticles [18,19] on various nanocarriers, including carbon nanotubes [20,21], graphene [22], magnetic beads [23], nanoparticles [10,24] and mesoporous materials [25]. Single-walled carbon nanohorn (SWCNH), a dahlia flowerlike nanostructure composed of thousands of graphitic tubule closed ends [26,27], possesses unique features of large surface area, plentiful inner nanospaces, highly defective horns, and good electrical conductivity [28,29], and has been used as an excellent nanocarrier to load high amount of gold nanoparticles (AuNPs) for signal amplification [19]. This work synthesized a nanogold loaded carbon nanohorn by in situ growth of nanogold on carboxylated CNH, and then functionalized it with streptavidin to design a signal tag (SA/Au/CNH) for recognizing the biotinylated signal antibody. This tag showed good stability and dispersibility in physiological buffer, and could serve as a common tracing tag to perform multiplexed immunoassay by electrochemical stripping analysis.

Different from the stripping analysis of quantum dots (QD) for enzyme-free electrochemical immunoassay [30,31], the stripping analysis of metallic nanoparticles, such as AuNPs [19,32] and silver nanoparticles (AgNPs) [16,33–36], can be performed by their direct electrochemical oxidiation in HCl to produce a detectable signal [14]. In comparison with AuNPs, AgNPs can be electrochemically oxidized at a relatively negative potential with a relatively sharp peak, thus, they are the more favorable signal tag than AuNPs. In addition, AgNP can be easily amplified by combining an in situ AuNP catalyzed enhancement [36]. This work combined the SA/Au/CNH tag with the nanomaterial-promoted silver enhancement to amplify the signal of stripping analysis. The combination improved greatly the analytical sensitivity. Using α-fetoprotein (AFP) and carcinoembryonic antigen (CEA) as model analytes and a disposable screen-printed electrode strip for preparation of immunosensor array, this method could detect these biomarkers down to 0.024 and 0.032 pg mL^{-1}, respectively. The localized silver deposition and electrochemical stripping detection eliminated completely signal cross-talk between adjacent immunosensors and the interference of dissolved oxygen, showing great promise for multiplex detection and clinical diagnosis application.

2. Experimental

2.1. Materials and reagents

SWCNHs were kindly provided by Professor Iijima (Japan Science and Technology Agency). Mouse monoclonal anti-AFP (clone No. bsm-1621) and mouse monoclonal anti-CEA (clone No. bsm-1623) were purchased from Beijing Biosynthesis Biotechnology Co., Ltd. (Beijing, China). Biotinylated anti-CEA and anti-AFP, and CEA and AFP standard solutions were gained from commercial AFP and CEA kit, respectively, which were supplied by Fujirebio Diagnostics AB (Göteborg, Sweden). Streptavidin was purchased from Promega Co. (USA). Bovine serum albumin (BSA), poly (diallyldimethylammonium chloride) (PDDA) (20%, w/w in water, MW: 200,000–350,000), chitosan (CS, ≥85% deacetylation) and silver enhancer solution A (S5020) and B (S5145) were purchased from Sigma–Aldrich Chemical Co. (St. Louis, MO). Glutaraldehyde (GA, 25% aqueous solution) was purchased from Alfa Aesar (China Ltd.). Chloroauric acid ($HAuCl_4 \cdot 4H_2O$) and trisodium citrate were obtained from Shanghai Reagent Company (Shanghai, China). Sodium borohydride ($NaBH_4$) was obtained from Sinopharm Chemical Reagent Co., Ltd. (China).

Tris–HNO_3 buffer (10 mM, pH 7.4) was prepared and used as working solution. The Tris–HNO_3 containing 0.05% (w/v) Tween-20 and 5% (w/v) BSA were used as washing buffer and blocking buffer, respectively. A mixture solution of 20-fold diluted silver enhancer solution A and B was freshly prepared for silver deposition. Ultrapure water obtained from a Millipore water purification system (≥18 MΩ, Milli-Q, Millipore) was used in the whole assay. Clinical serum samples were from Jiangsu Institute of Cancer Research. All other reagents were of analytical grade and used as received.

2.2. Apparatus

The transmission electron micrographs (TEM) were gained on a JEM-2100 TEM (JEOL, Japan). The IR spectra were recorded using a NEXUS870 Fourier-transform infrared (FTIR) spectrometer (NICOLET, USA). The scanning electron micrographs (SEM) were obtained with a Hitachi S-4800 scanning electron microscope (Japan) at an acceleration voltage of 10 kV. All electrochemical immunoassays were performed on a CHI 660B electrochemical workstation (Chenhua, Shanghai, China).

2.3. Preparation of SA/Au/CNH nanocomplex

Carboxylic group-abundant SWCNHs were firstly obtained by dispersing SWCNHs in 30% HNO_3 and refluxing for 24 h at 140 °C. After centrifugation, the sediment was washed with water until the pH reached 7.0 and then dispersed in ultrapure water at the concentration of 1 mg mL^{-1}. The PDDA layer was then assembled on the carboxylated SWCNHs through adding 1 mL of 1 mg mL^{-1} carboxylated SWCNHs into 1 mL of 0.20% PDDA aqueous solution containing 0.5 M NaCl and stirring for 40 min. Residual PDDA was removed by centrifugation at 12,000 rpm, and the precipitate was redispersed in 8 mL water.

The Au/CNH was prepared by adding 20 μL of $HAuCl_4$ (25 mM) and 20 μL of 1% trisodium citrate into above polyelectrolyte functionalized SWCNH solution under vigorous stirring in an ice-water bath for 30 min, followed by addition of 50 μL of freshly prepared ice-cold $NaBH_4$ (0.1 M) and vigorous stirring for 2 min. The resulting Au/CNH was collected by centrifugation (5500 rpm) and washing with water, then dispersed in 4 mL of 10 mM pH 9.0 Tris–HNO_3.

10 μL of 1.0 mg mL^{-1} streptavidin was finally added into 400 μL of Au/CNH suspension, followed by gently stirring in room temperature for 1 h. The resulting mixture was centrifuged at 3800 rpm for 10 min at 4 °C. The sediment was washed three times with pH 7.4 Tris–HNO_3 buffer to remove the unconjugated streptavidin and then dispersed in 400 μL of pH 7.4 Tris–HNO_3 containing 1% BSA at 4 °C for 0.5 h to block the remaining exposed surface of nanogolds. Following a centrifugation at 3500 rpm for 10 min, the resulting SA/Au/CNH nanocomplex was dispersed in 400 μL of 10 mM pH 7.4 Tris–HNO_3 containing 0.1% BSA.

2.4. Preparation of immunosensor array

The screen-printed carbon electrodes (SPCEs) containing two graphite working electrodes (W_1 and W_2, diameter: 2 mm), a

Ag/AgCl reference electrode, and a graphite auxiliary electrode were prepared according to our previous report [37]. 1.5 μL of 0.25 mg mL^{-1} chitosan was coated on each working electrode and dried at room temperature. After activating with 2.5% glutaraldehyde for 2 h and washing with water, 1.0 μL of 0.2 mg mL^{-1} anti-AFP and anti-CEA capture antibodies were dropped onto the corresponding working electrodes and reacted at room temperature for 60 min and then 4 °C overnight in a 100% moisture-saturated environment. Subsequently, the excessive antibodies were washed out with washing buffer and pH 7.4 Tris–HNO_3. Finally, 20 μL of blocking solution was dropped on the working electrodes and incubated for 60 min at room temperature to block possible remaining active sites against nonspecific adsorption. After washing with washing buffer and pH 7.4 Tris–HNO_3, the immunosensor array was obtained.

2.5. Immunoassay procedure

The immunoassay procedure is shown in Scheme 1. The immunosensor array was first incubated with 15 μL of the mixture of AFP and CEA standard solutions or serum samples for 30 min at 37 °C. After a washing step, 15 μL of the mixture of biotinylated anti-AFP and biotinylated anti-CEA at the concentration of 0.5 μg mL^{-1} was dropped onto the immunosensor array and incubated for 30 min at 37 °C. Following another washing step, 15 μL of the SA/Au/CNH nanocomplex was dropped onto the immunosensor array and incubated for 15 min at 37 °C. After a washing step, silver deposition was performed using 15 μL of silver deposition solutions for 6 min at 37 °C in a dark incubator, followed by rinsing with water. Subsequently, linear sweep voltammetry (LSV) was performed from −0.15 to 0.3 V at 50 mV s^{-1} in 1.0 M KCl solution to record the stripping currents at W_1 and W_2 for simultaneous detection of AFP and CEA.

3. Results and discussion

3.1. Characterization of SA/Au/CNH nanocomplex

TEM was used to characterize the formation of Au/CNH. After oxidation treatment, the carboxylated SWCNHs maintained the dahlia-like nanostructure with a diameter of about 80–100 nm (Fig. 1A). Using positively charged PDDA as a bridge, the $AuCl_4^-$ could be electrostatically absorbed on the surface of SWCNHs to produce nanogold by chemical reduction. As shown in Fig. 1B, numerous nanoparticles with a diameter of about 7 nm were uniformly distributed on the surface of CNH, indicating the successful synthesis of Au/CNH.

The Au/CNH could be easily functionalized with streptavidin via the inherent interaction between amine or SH groups of protein and nanogold [38] to form SA/Au/CNH. The FTIR spectrum of Au/CNH displayed two peaks at 1585 and 1728 cm^{-1} (Fig. 1C, curve a), which were assigned to the carbonyl stretch mode of the carboxylated CNH [39]. In contrast, the FTIR spectrum of SA/Au/CNH showed two obvious absorption peaks corresponding to the amide bands I (1649 cm^{-1}) and II (1550 cm^{-1}) (Fig. 1C, curve b) of streptavidin [34], indicating the successful conjugation of streptavidin with Au/CNH. Because of the negatively charged character of streptavidin, the obtained SA/Au/CNH nanocomplex could be well dispersed in a physiological buffer (Fig. 1D), which was very favorable for their further application in bioassays.

3.2. Characterization of immunoassay and signal amplification by SA/Au/CNH tag

SEM was used to characterize the surface morphologies of immunosensor before and after the sandwich immunoreaction and in situ silver deposition. After coating CS on the working electrodes, smooth and uniform surface could be formed (Fig. 2A). When the capture antibody was immobilized on the CS modified electrode by glutaraldehyde cross-linking, an obvious aggregation of the trapped biomolecules was observed (Fig. 2B). Through a sandwich-type immunoreaction, the immmunocomplex was generated on the immunosensor surface. Upon the biotin-streptavidin recognition, the SA/Au/CNH was bound on the immunocomplex, and the denser aggregation of the biomolecules was observed on the surface (Fig. 2C). The further silver deposition led to the aggregation of AgNPs on the surface of CNH. The resulting nanostructure with a diameter of about 500–800 nm maintained the dahlia-like shape of CNH (Fig. 2D).

In order to evaluate the amplification ability of SA/Au/CNH tag, the sandwich immunoassays of 0.1 ng mL^{-1} AFP with SA/Au/CNH or SA/Au as tag were performed. In the presence of SA/Au/CNH tag, the response of 24.1 μA was two times higher than that using SA/Au as the tag, indicating the more efficient amplification of silver deposition on SA/Au/CNH tag (Fig. 3A). It was noted that a signal of 6.7 μA was observed without any tag. This response was similar to the background signal (Fig. 3B), and should be resulted from the chemical reduction of Ag^+ in the absence of AuNPs.

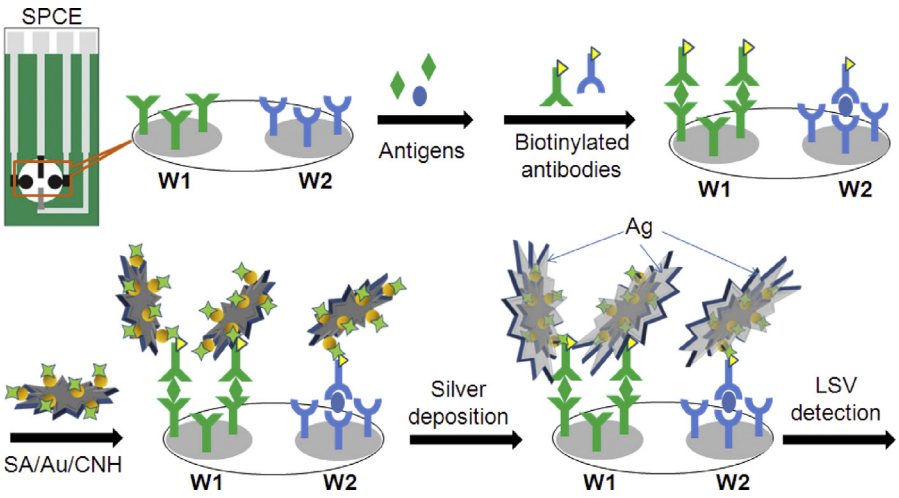

Scheme 1. Schematic representation of sandwich-type immunoassay procedure.

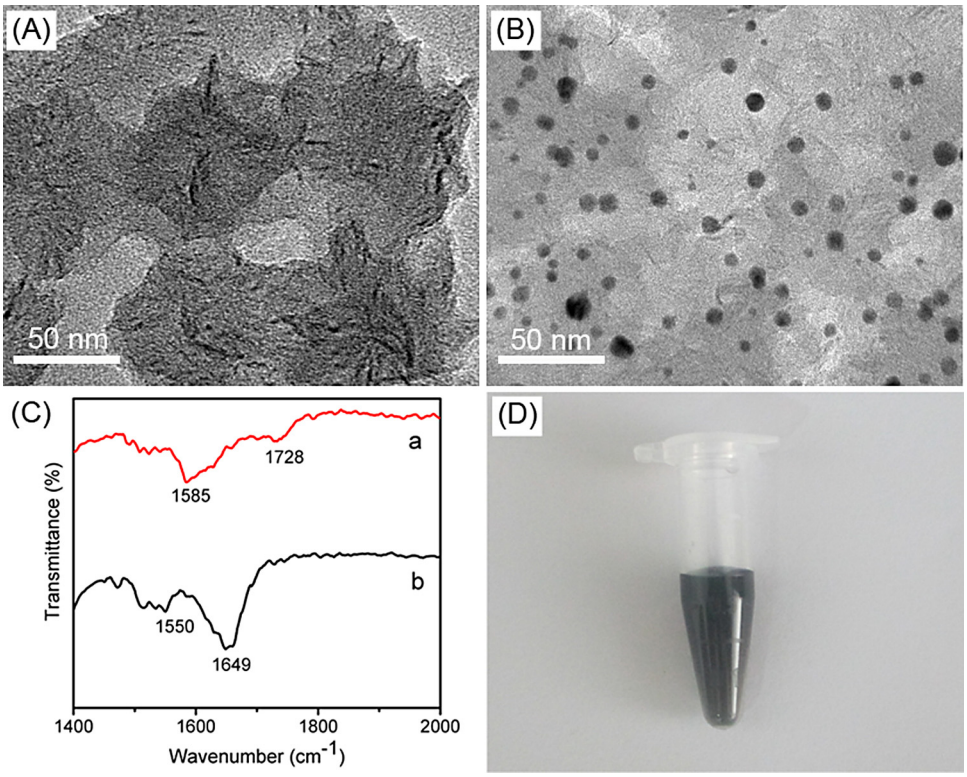

Fig. 1. (A) TEM image of SWCNHs, (B) TEM image of Au/CNH, (C) FTIR spectra of Au/CNH (a) and SA/Au/CNH (b), and (D) photograph of SA/Au/CNH suspension.

3.3. Optimization of detection conditions

The deposited AgNPs on the immunosensor array could be easily detected by anodic stripping voltammetric analysis. During a linear potential sweep, the deposited AgNPs showed a well-defined anodic stripping peak at the peak potential of 0.048 V, which was more negative than that reported previously [40] due to the presence of Cl^-. The peak current increased with

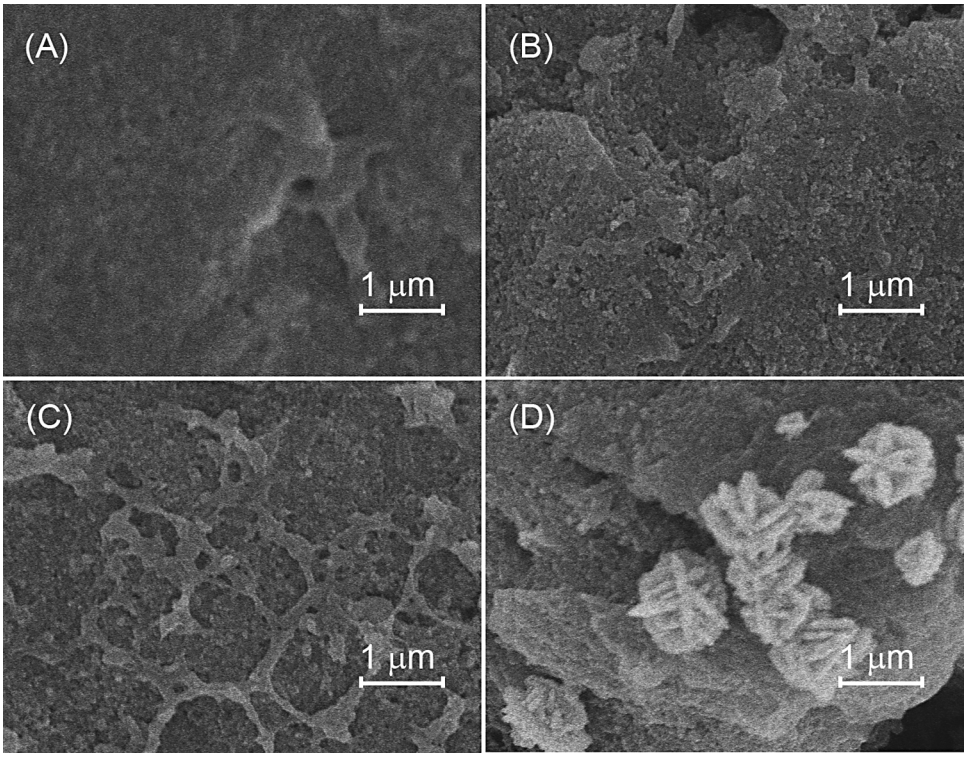

Fig. 2. SEM images of (A) CS modified SPCE, immunosensor (B) with the formation of sandwich immunocomplex and conjugation of SA/Au/CNH (C), followed by silver-deposition (D).

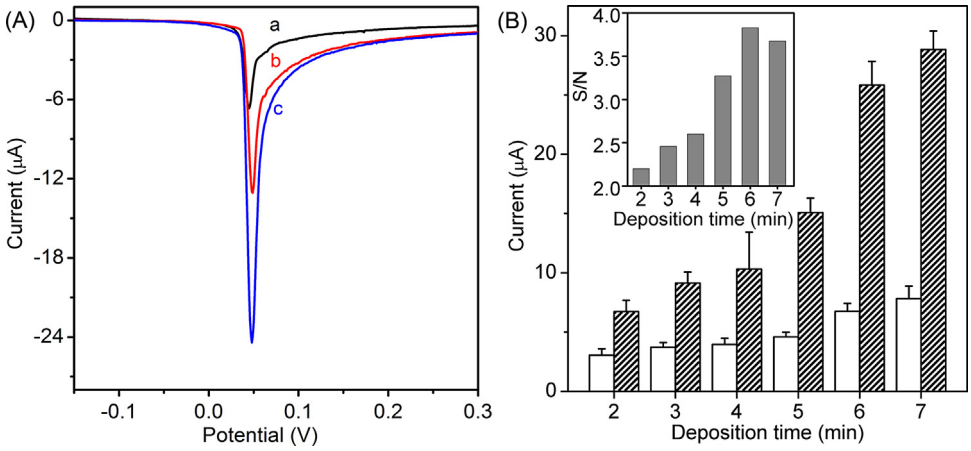

Fig. 3. (A) Stripping voltammetric responses of the immunosensor in 1.0 M KCl after sandwich immunoreaction with 0.1 ng mL^{-1} AFP without (a) and with SA/Au (b) and SA/Au/CNH (c) as tag for 6 min silver deposition at 37 °C. (B) Effects of silver deposition time on stripping currents of AgNPs in 1.0 M KCl for blank control (white column) and 0.5 ng mL^{-1} AFP (diagonal filled column). Inset: ratios of signal to control at different deposition times.

the increasing concentration of antigen used in the sandwich immunoreaction, and could thus be used for immunoassay.

Obviously, the amount of deposited AgNPs on the surface of SPCEs depended on the concentration of silver enhancer solution and deposition time. At 20-fold dilution of silver enhancer condition, the stripping current of deposited AgNPs greatly increased with the increasing of deposition time, while the longer deposition time led to higher background current due to the spontaneous chemical reduction of Ag^+ in the absence of AuNPs (Fig. 3B). To obtain higher sensitivity, the maximum ratio of signal to noise was used to choose the optimum condition. As shown in inset in Fig. 3B, the optimum deposition time was 6 min.

3.4. Evaluation of cross-reactivity and cross-talk

To investigate the cross-reactivity between analytes and non cognate antibodies, the silver stripping currents on the immunosensor array incubated with blank solution, 0.5 ng mL^{-1} AFP, 0.5 ng mL^{-1} CEA, and the mixture of 0.5 ng mL^{-1} AFP and CEA were compared. As expected, both the AFP and the CEA immunosensors showed obvious stripping responses only toward their corresponding proteins (Fig. 4). Apparently, the cross-reactivity at the array was negligible. In addition, no substrate or mediator was required in the detection procedure, and the silver-deposition enhancement and stripping analysis occurred only on the corresponding immunosensor surface. Therefore, no electrochemical cross-talk occurred among neighboring electrodes, and simultaneous multianalyte immunoassay could be performed in a single run using the immunosensor array.

3.5. Analytical performance

Under the optimum conditions, the stripping peak current of the deposited AgNPs on the immnuosensor array for simultaneous detection of AFP and CEA increased proportionally with the increasing concentration of analytes. Both calibration plots showed good linear relationships between the peak currents and the logarithm values of the analyte concentrations in the range from 0.1 pg mL^{-1} to 1.0 ng mL^{-1} (Fig. 5). The correlation coefficients were 0.9992 and 0.9983 for AFP and CEA, respectively. The limits of detection for AFP and CEA were 0.024 and 0.032 pg mL^{-1}, respectively, which were much lower than those reported in the previous studies [34,41,42].

Both the intra-assay and the inter-assay precisions of the immunosensor array were examined by parallel immunoassay for 5 times with the mixture of 0.5 ng mL^{-1} AFP and CEA solutions. The intra-assay relative standard deviations (RSD) were 3.80% and 3.69% for AFP and CEA, and the inter-assay RSD were 4.04% and 4.34%, respectively. The results showed that the immunosenor arrays had good precision and acceptable fabrication reproducibility. In addition, after the immunosensor arrays were stored dry at 4 °C for 1 week, 95.58% and 94.82% of the initial responses for AFP and CEA was remained, respectively. The results indicated that the immunosensor array had acceptable stability.

3.6. Application in analysis of serum samples

To evaluate the reliability and application potential of the proposed immunoassay method, the assay results of AFP and CEA in human serum samples using the proposed method were compared with the reference values obtained by commercial electrochemiluminescent single-analyte tests. The results are listed in Table 1. Acceptable results with relative errors less than

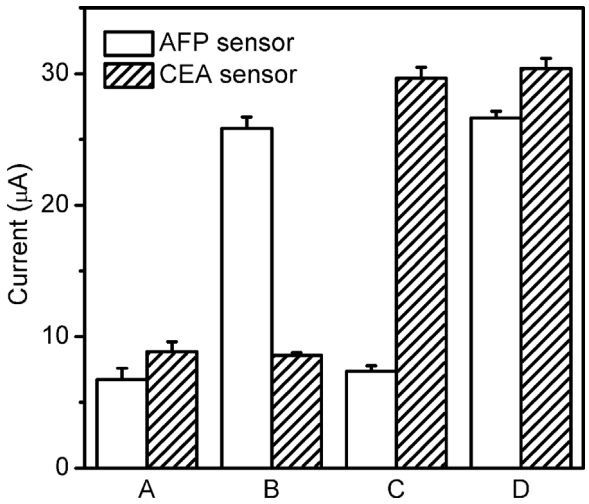

Fig. 4. LSV responses of AgNPs on the immunosensor array incubated with (A) blank control, (B) 0.5 ng mL^{-1} AFP, (C) 0.5 ng mL^{-1} CEA and (D) the mixture of 0.5 ng mL^{-1} AFP and CEA solution.

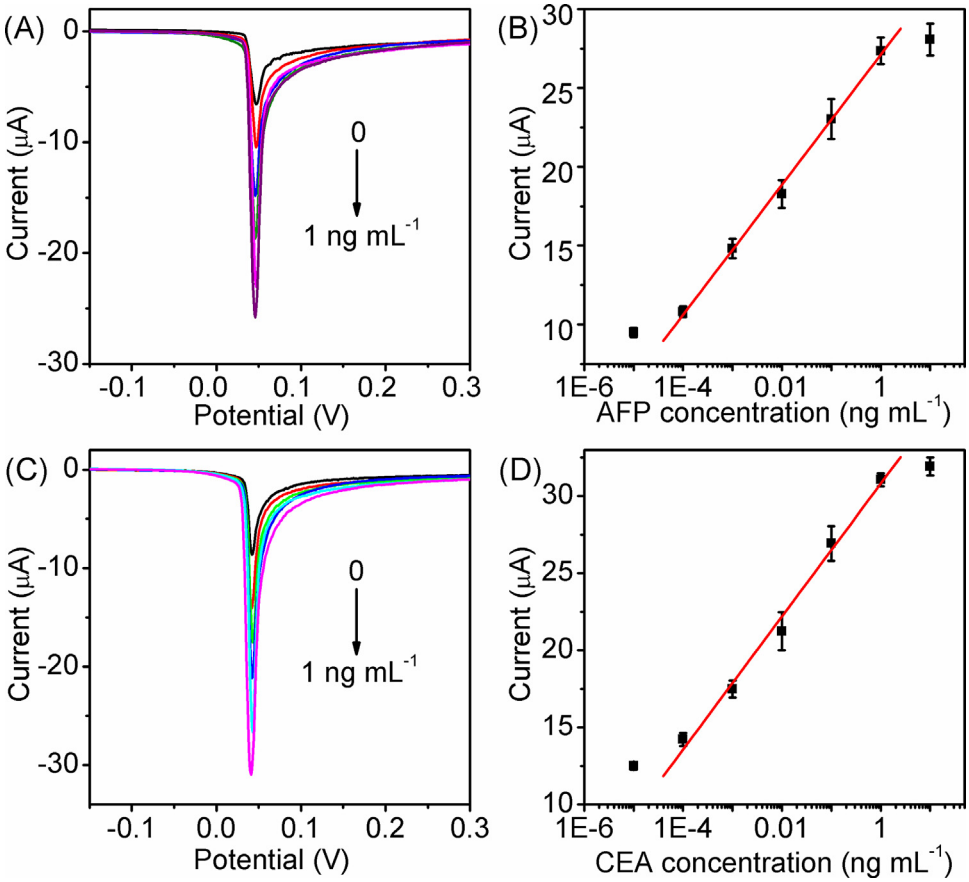

Fig. 5. LSV curves of AgNPs (A and C) and calibration curves (B and D) for simultaneous multiplexed detection of AFP (A and B) and CEA (C and D).

Table 1
Assay results of clinical serum samples using the proposed and reference methods.

Serum samples	AFP			CEA		
	Proposed method (pg mL^{-1})[a]	Reference method[b] (ng mL^{-1})	Relative error (%)	Proposed method (pg mL^{-1})[a]	Reference method (ng mL^{-1})	Relative error (%)
1	21.4	2.21	−3.16	25.7	2.54	1.18
2	44.9	4.32	3.94	73.1	6.86	6.56
3	29.4	3.2	−8.13	37.7	3.6	4.72

[a] The serum samples were diluted at 100 times prior to assay using the proposed method.
[b] The reference values were obtained from electrochemiluminescent single-analyte tests on commercial automation electrochemiluminescent analyzer (Elecsys 2010, Roche) and supplied by Jiangsu Institute of Cancer Prevention and Cure.

8.13% indicated good accuracy of the proposed method for the detection of clinical samples.

4. Conclusions

A novel Au/CNH nanostructure has been prepared by one-pot in situ growth of nanogold on carboxylated single-walled CNH. It can be easily functionalized with streptavidin for preparation a common tracing tag to perform multiplexed sandwich-typed immunoassay using biotinylated signal antibodies. Combined with a disposable immunosensor array and a nanogold-promoted AgNPs deposition process, an ultrasensitive multiplexed immunosensing method is proposed. With the electrochemical stripping analysis of the deposited AgNPs, the proposed method shows a wide detection range and an ultralow detection limit for both AFP and CEA. Besides, the detection step excludes the deoxygenation procedure and cross-talking. The multiplexed immunoassay is designed with a sandwich assay format on a disposable screen-printed carbon electrode array, along with high detection sensitivity and acceptable accuracy, thus, shows great promise in clinical application.

Acknowledgements

This work was financially supported by National Basic Research Program of China (2010CB732400), the National Science Fund for Creative Research Groups (21121091), the National Natural Science Foundations of China (21135002, 21075055 and 21105046), and Natural Science Foundation of Jiangsu (BK2010302 and BK2011552).

References

[1] D. Sidransky, Nat. Rev. Cancer 2 (2002) 210.
[2] J. Wu, Z.F. Fu, F. Yan, H.X. Ju, Trends Anal. Chem. 26 (2007) 679–688.
[3] K. Kojima, A. Hiratsuka, H. Suzuki, K. Yano, K. Ikebukuro, I. Karube, Anal. Chem. 75 (2003) 1116.
[4] M.S. Wilson, W.Y. Nie, Anal. Chem. 78 (2006) 2507.
[5] J. Wu, F. Yan, J.H. Tang, C. Zhai, H.X. Ju, Clin. Chem. 53 (2007) 1495.
[6] G.F. Zheng, F. Patolsky, Y. Cui, W.U. Wang, C.M. Lieber, Nat. Biotechnol. 23 (2005) 1294.
[7] F. Deiss, C.N. Lafratta, M. Symer, T.M. Blicharz, N. Sojic, D.R. Walt, J. Am. Chem. Soc. 131 (2009) 6088.
[8] M. Hu, J. Yan, Y. He, H.T. Lu, L.X. Weng, S.P. Song, C.H. Fan, L.H. Wang, ACS Nano 4 (2010) 488.
[9] M.H. Kwon, D.H. Kong, S.H. Jung, I.B. Suh, Y.M. Kim, K.S. Ha, Anal. Chem. 83 (2011) 2317.
[10] C. Zong, J. Wu, C. Wang, H.X. Ju, F. Yan, Anal. Chem. 84 (2012) 2410.
[11] B. Qu, L. Guo, X. Chu, D.H. Wu, G.L. Shen, R.Q. Yu, Anal. Chim. Acta 663 (2010) 147.
[12] Y.Y. Cai, H. Li, B. Du, M.H. Yang, Y. Li, D. Wu, Y.F. Zhao, Y.X. Dai, Q. Wei, Biomaterials 32 (2011) 2117.
[13] Y. Xie, A. Chen, D. Du, Y. Lin, Anal. Chim. Acta 699 (2011) 44.
[14] X.M. Pei, B. Zhang, J. Tang, B.Q. Liu, W.Q. Lai, D.P. Tang, Anal. Chim. Acta 758 (2013) 1.
[15] D. Du, Z.X. Zou, Y. Shin, J. Wang, H. Wu, M.H. Engelhard, J. Liu, I.A. Aksay, Y.H. Lin, Anal. Chem. 82 (2010) 2989.
[16] W.Q. Lai, D.P. Tang, X.H. Que, J.Y. Zhuang, L.B. Fu, G.N. Chen, Anal. Chim. Acta 755 (2012) 62.
[17] G.Q. Sun, J.J. Lu, S.G. Ge, X.R. Song, J.H. Yu, M. Yan, J.D. Huang, Anal. Chim. Acta 775 (2013) 85.
[18] Y.F. Wu, P. Xue, Y.J. Kang, K.M. Hui, Anal. Chem. 85 (2013) 3166.
[19] C.R. Zhao, D.J. Lin, J. Wu, L. Ding, H.X. Ju, Electroanalysis 25 (2013) 1044.
[20] X. Yu, B. Munge, V. Patel, G. Jensen, A. Bhirde, J.D. Gong, S.N. Kim, J. Gillespie, J.S. Gutkind, F. Papadimitrakopoulos, J.F. Rusling, J. Am. Chem. Soc. 128 (2006) 11199.
[21] G.S. Lai, F. Yan, H.X. Ju, Anal. Chem. 81 (2009) 9730.
[22] D. Du, L.M. Wang, Y.Y. Shao, J. Wang, M.H. Engelhard, Y.H. Lin, Anal. Chem. 83 (2011) 746.
[23] V. Mani, B.V. Chikkaveeraiah, V. Patel, J.S. Gutkind, J.F. Rusling, ACS Nano 3 (2009) 585.
[24] Y.F. Wu, C.L. Chen, S.Q. Liu, Anal. Chem. 81 (2009) 1600.
[25] M. Hasanzadeh, N. Shadjou, M. Eskandani, M.D.L. Guardia, E. Omidinia, Trends Anal. Chem. 45 (2013) 93.
[26] R. Yuge, T. Ichihashi, Y. Shimakawa, Y. Kubo, M. Yudasaka, S. Iijima, Adv. Mater. 16 (2004) 1420.
[27] M.F. Zhang, T. Yamaguchi, S. Iijima, M. Yudasaka, J. Phys. Chem. C 113 (2009) 11184.
[28] C. Yang, H. Noguchi, K. Murada, M. Yudasaka, A. Hashimoto, S. Iijima, K. Kaneko, Adv. Mater. 17 (2005) 866.
[29] K.M. Urita, S. Seki, S. Utsumi, D. Noguchi, H. Kanoh, H. Tanaka, Y. Hattori, Y. Ochiai, N. Aoki, M. Yudasaka, S. Iijima, K. Kaneko, Nano Lett. 6 (2006) 1325.
[30] G.D. Liu, J. Wang, J. Kim, M.R. Jan, Anal. Chem. 76 (2004) 7126.
[31] L.Y. Chen, C.L. Chen, R.N. Li, Y. Li, S.Q. Liu, Chem. Commun. 19 (2009) 2670.
[32] J.A. Ho, H.C. Chang, N.Y. Shih, L.C. Wu, Y.F. Chang, C.C. Chen, C. Chou, Anal. Chem. 82 (2010) 5944.
[33] B.P. Ting, J. Zhang, M. Khan, Y.Y. Yang, J.Y. Ying, Chem. Commun. (2009) 6231.
[34] G.S. Lai, J. Wu, H.X. Ju, F. Yan, Adv. Funct. Mater. 21 (2011) 2938.
[35] Y. Wan, Y. Wang, J.J. Wu, D. Zhang, Anal. Chem. 83 (2011) 648.
[36] X. Chu, X. Fu, K. Chen, G.L. Shen, R.Q. Yu, Biosens. Bioelectron. 20 (2005) 1805.
[37] J. Wu, J.H. Tang, Z. Dai, F. Yan, H.X. Ju, N.E. Murrc, Biosens. Bioelectron. 22 (2006) 102.
[38] C. Sönnichsen, B.M. Reinhard, J. Liphardt, A.P. Alivisatos, Nat. Biotechnol. 23 (2005) 741.
[39] J. Zhang, J.P. Lei, C.L. Xu, L. Ding, H.X. Ju, Anal. Chem. 82 (2010) 1117.
[40] H. Li, Z.Y. Sun, W.Y. Zhong, N. Hao, D.K. Xu, H.Y. Chen, Anal. Chem. 82 (2010) 5477.
[41] Z.J. Song, R. Yuan, Y.Q. Zhai, Y. Zhuo, W. Jiang, H.L. Su, X. Che, J.J. Li, Chem. Commun. 46 (2010) 6750.
[42] J.H. Lin, Z.J. Wei, C.M. Mao, Biosens. Bioelectron. 29 (2011) 40.